Estimating Soil Moisture and Electrical Conductivity Using Wi-Fi

Jian Ding
Microsoft Research

Ranveer Chandra
Microsoft Research

Abstract

Soil Moisture and Soil Electrical Conductivity (EC) are important parameters for data-driven farming. This knowledge can help a farmer improve crop yield, reduce input costs, and adopt sustainable agriculture practices. However, the high cost of commercial soil moisture and EC sensors has limited their adoption. In this paper, we present the design and implementation of a system, called SMURF, that senses soil moisture and soil EC using RF propagation in existing Wi-Fi bands. It overcomes the key challenge of limited bandwidth availability in the 2.4 GHz unlicensed spectrum using a novel multi-antenna technique that maps the propagation time and amplitude of Wi-Fi to the different antennas as a function of the refractivity and permittivity of soil, and uses them to infer soil moisture and EC. Our experiments with software defined radios (USRP and WARP), and two commodity Wi-Fi cards show that SMURF can accurately estimate soil moisture and EC using Wi-Fi, thereby enabling a future in which a farmer with a smartphone that has a Wi-Fi radio can sense soil in her farm without investing 100s of dollars in soil sensing equipment.

1 Introduction

Several agricultural applications rely on soil moisture and soil EC measurements. For example, precision irrigation, which refers to the variable application of water in different regions of the farm, depends on accurate soil moisture values at different depths. This helps reduce the amount of water use, and also reduces the leeching of ground water by the contaminants used in fertilizers and other agricultural inputs. Soil EC is another key indicator of soil health. It has been shown to correlate very well with crop yield and plant nutrient availability, and farmers are recommended by the USDA to measure soil EC to determine soil treatment plans and management zones for Precision Agriculture [1].

Several techniques have been invented over the last few decades to measure soil moisture and EC. These methods include direct sensing techniques, that require soil to be extracted and dried out, as well as indirect sensing methods that measure surrogate properties of soil moisture and EC, such as capacitance, electrical, and nuclear response. Researchers have also explored the use of radar based technologies to measure soil moisture and EC.

However, one of the key challenges in the adoption of soil moisture and EC sensing technologies is the cost of existing sensor solutions. Although hobbyist soil moisture sensors are available for less than 10 dollars, they are not reliable and degrade quickly, and are consequently not used by agricultural experts [2]. We are not aware of any low cost soil EC sensor. The lowest cost, commercial grade, soil moisture or soil EC sensing solutions still cost over a 100 dollars. They use ruggedized components that typically measure the resistance, capacitance, or conductivity change of the sensor (discussed in Section 2). The cost of the sensor package is further increased by the need for additional components, such as the microprocessor, ADC, cables, packaging, etc.

At these price points for soil sensors, it is unaffordable for most farmers to adopt moisture or EC sensing technologies. Most farmers in developing regions don't make enough to afford sensors that cost a few hundred dollars. In fact, even in the developed world, the cost of these sensors has limited the adoption of precision irrigation technologies [3].

In this paper we present a low-cost soil sensing technique called SMURF, for Soil Measurements Using RF, that estimates soil moisture and soil EC without the need for a specialized sensor. Instead, SMURF leverages the phenomenon that *RF waves travel slower in soil with higher permittivity*. With just a few antennas in soil, SMURF can estimate the permittivity, and the corresponding moisture and EC levels of soil at the location of the antennas.

Even though prior work on Ground Penetrating Radars (GPRs) has considered using RF for measuring soil properties, these systems are specialized, wideband (a few GHz in the lower UHF spectrum), and hence cost several 1000s of dollars. In contrast, SMURF uses Wi-Fi devices in the unlicensed 2.4 GHz of spectrum, with multiple antennas placed

at different depths in the soil. A wireless transmitter, e.g. Wi-Fi, from the soil surveying device, emits signals that are received by these antennas in soil. The receiver uses signals on multiple antennas to compute soil permittivity. The results are then transmitted back to the soil surveying device, which then computes the soil moisture and soil EC values at the location of the antenna.

This capability of SMURF enables several new scenarios. For example, a farmer with a Wi-Fi enabled smartphone will be able to learn about the soil in their farm. A tractor or a UAV (unmanned aerial vehicle) can create new up to date maps of the soil every time they traverse the farm. An EC map can help a farmer build management zones. A sprinkler system can dynamically learn of moisture maps of the farm, and adapt the time of irrigation, and the amount of water that it uses in different regions. And there are many more.

Previous GPR techniques use time of flight (ToF) to measure the speed of the RF signal, and consequently the permittivity of soil. They use wideband spectrum from 100s of MHz to few GHz of spectrum to measure ToF. However, such a wide contiguous bandwidth is not available in the unlicensed spectrum. Furthermore, time of flight measures the average moisture level from the surface of soil, but doesn't measure the absolute moisture levels, such as the soil moisture 8 inches below surface level.

SMURF addresses the above challenges by proposing a new technique to estimate the moisture and EC level from Wi-Fi signals. Due to poor propagation in 5 GHz of spectrum, SMURF only uses the 70 MHz of available spectrum in 2.4 GHz. Instead of measuring the absolute ToF, which would require a wide bandwidth, SMURF uses a technique to measure the relative ToF of the received signal between multiple antennas. The relative ToF is used to determine the permittivity and soil moisture. We then propose a new technique to measure soil EC using the ratio of signal amplitudes on the different antennas.

To the best of our knowledge, SMURF is the first work to demonstrate how Wi-Fi transmissions in the unlicensed spectrum can be used to sense soil moisture and soil EC. We have implemented SMURF in the 2.4 GHz unlicensed bands over various hardware, including USRP, WARP, and Intel and Qualcomm Atheros based Wi-Fi cards, and shown the system to perform as well as the more expensive soil sensors.

Furthermore, through this design, this paper makes the following contributions:

- It shows how average soil moisture from the surface of soil to the antenna can be estimated using a narrow bandwidth in the unlicensed spectrum by leveraging machine learning models trained on CSI, along with a combination of other RF parameters.
- It presents a new technique to estimate soil moisture at a given depth by mapping it to the permittivity and refractive index of soil, and approximating it using the time difference of arrival between antennas.
- It presents a new technique to estimate soil EC using relative amplitudes of signals received by multiple antennas.
- It solves systems challenges related to antenna placement in soil, and fast (joint) estimation of average moisture from surface level to the antenna, along with moisture level at the location of the antenna.
- It demonstrates how the system can be implemented in the 2.4 GHz unlicensed bands, and over various hardware, such as USRP, WARP, and Intel and Qualcomm Atheros based Wi-Fi cards.

2 Background

We first provide some background on the state of the art in soil moisture and EC sensing, and then show how GPR based techniques have used RF for estimating soil moisture.

2.1 Sensing Soil Moisture and EC

The most accurate method for soil sensing is the direct gravimetric method [4]: of sampling soil, drying it out, and weighing the amount of moisture that is lost from the soil. However, this technique is expensive, manual, requires oven drying, and disturbs the soil.

Several lower-cost surrogate sensing approaches have been proposed in the literature that estimate soil moisture based on the indirect properties of soil that are affected by moisture. For example, electrical resistance based sensors measure the resistance of soil when current is passed through two electrodes [5]. Capacitive sensors measure the time to charge the capacitor. A calibration chart is then used to convert the resistance to the corresponding soil moisture value. Heat-diffusion sensors measure the rate of increase of temperature when applying a heat source [6]. Wet soil dissipates heat much faster than dry soil. Tensiometers [7] measure the tension created by soil absorbing the water kept in a ceramic cup connected through a tube. Radioactive sensors [8] measure the slowing of neutrons in soil after being emitted into the soil from a fast-neutron source. Most "commercial" grade soil moisture sensors, such as the ones from Decagon, Campbell Scientific, or Sensoterra, typically cost over a 100 dollars.

To measure EC, the resistance to current is measured through electrodes in soil. The most inexpensive sensors we are aware of cost over a 100 dollars. They have to be to connected to a microprocessor and RF modules, and hence are even more expensive.

2.2 Soil Sensing Using RF

ToF-based RF sensing techniques, such as GPRs and TDRs, exploit the relationship between electromagnetic (EM) wave characteristics and material properties. Two key material properties that enable RF-based sensing are dielectric permittivity and electrical conductivity (EC). Compared with wave propagation in free space, larger permittivity and EC values in soils add attenuation to the signal strength and slows down the wave propagation speed. Conversely, knowing the attenuation and velocity of a signal traveling in a soil can help to figure out the permittivity and EC of that soil. Next, we will mathematically explain the relationship between material properties and wave propagation.

Permittivity, $\varepsilon^* = \varepsilon^{'} + j\varepsilon^{''}$, is a complex value, where $\varepsilon^{'}$ and $\varepsilon^{''}$ are its real and complex components. It is usually represented by the the term relative permittivity given as:

$$\varepsilon_r^* = \frac{\varepsilon^*}{\varepsilon_0} = \frac{\varepsilon^{'}}{\varepsilon_0} + j\frac{\varepsilon^{''}}{\varepsilon_0} = \varepsilon_r^{'} + j\varepsilon_r^{''} \tag{1}$$

where ε_0 is the permittivity of free space (8.854×10^{-12} F/m). EC is usually represented by a real value, σ, since its imaginary component is insignificant at radio frequencies. Permittivity (in F/m) and EC (in S/m) affect attenuation and phase rotation for a signal that propagates in a conducting dielectric medium at frequency f and travels a distance of d in the following form:

$$E(f,d) = \frac{A}{d} e^{-(\alpha + j\beta)d} \tag{2}$$

where

$$\alpha = \frac{2\pi f}{c} \sqrt{\frac{\varepsilon_r^{'}}{2}\left[\sqrt{1 + \left(\frac{\varepsilon_r^{''} + \frac{\sigma}{2\pi f \varepsilon_0}}{\varepsilon_r^{'}}\right)^2} - 1\right]} \tag{3}$$

$$\beta = \frac{2\pi f}{c} \sqrt{\frac{\varepsilon_r^{'}}{2}\left[\sqrt{1 + \left(\frac{\varepsilon_r^{''} + \frac{\sigma}{2\pi f \varepsilon_0}}{\varepsilon_r^{'}}\right)^2} + 1\right]} \tag{4}$$

are the attenuation coefficient that determines signal attenuation and phase coefficient that determines phase variation during propagation. c is the speed of light and A is the signal amplitude determined by wavelength in the medium and system parameters including antenna beam pattern, gain settings at transmitter and receiver, and antenna gains. For isotropic antennas, A is given as follows from the Friis equation [9]:

$$A = \frac{\sqrt{P_r G_t G_r}\lambda}{4\pi} \tag{5}$$

where P_r is the transmit power, G_t and G_r are the transmit and receive antenna gains. Compared with wave propagation in free space, which is given as:

$$E_0(f,d) = \frac{A_0}{d} e^{\frac{j2\pi fd}{c}} = \frac{\lambda_0 A}{\lambda d} e^{-(\alpha_0 + j\beta_0)d} \tag{6}$$

where $\alpha_0 = 0$ and $\beta_0 = 2\pi f/c$, we can see that the dielectric medium basically adds an extra attenuation due to the change of wavelength λ_0/λ and the transmission loss $e^{\alpha d}$, and slows down the speed of wave by a factor of β/β_0. The propagation velocity can be expressed as follows:

$$v = \frac{c}{\beta/\beta_0} = \frac{c}{\sqrt{K_a}} \tag{7}$$

where

$$K_a = \frac{\varepsilon_r^{'}}{2}\left[\sqrt{1 + \left(\frac{\varepsilon_r^{''} + \frac{\sigma}{2\pi f \varepsilon_0}}{\varepsilon_r^{'}}\right)^2} + 1\right] \tag{8}$$

is known as the apparent permittivity of a material, which is often adopted in ToF-based RF techniques to describe the permittivity estimated from ToF. When $\varepsilon_r^{''}$ and $\sigma/2\pi f\varepsilon_0$ are small compared with $\varepsilon_r^{'}$, the above equation reduces to:

$$K_a = \varepsilon_r^{'} \tag{9}$$

The typical range of $\sqrt{K_a}$ in soil is 2-6, corresponding to 2-6 times slow down of wave speed in soil compared with the speed of light [10].

2.2.1 Water Content Estimation from ToF

ToF-based RF techniques measure ToF to estimate wave velocity v and then determine the apparent permittivity K_a of soil. The relationship between K_a and ToF of a signal traveling through a known distance d is given as follows:

$$K_a = \left(\frac{c\tau}{d}\right)^2 \tag{10}$$

Soil is considered as a mixture of soil particles, water and air. The permittivity of soil strongly depends on the water content in it since water has a much larger permittivity than air and soil particles. The permittivity of water is around 80, while the permittivity of air is 1 and the permittivity of soil particles is from 3 to 10. The water content-permittivity relationship of soils has been well studied and modeled [11, 12, 13]. Once the permittivity value of a soil is obtained, it can be fit into existing water content-permittivity models for that soil type to estimate the water content. An example model, which is widely used for mineral soils [11], is as follows:

$$\begin{aligned}\theta = &-5.3 \times 10^{-2} + 2.92 \times 10^{-2} K_a - 5.5 \times 10^{-4} K_a^2 \\ &+ 4.3 \times 10^{-6} K_a^3\end{aligned} \tag{11}$$

where θ is the volumetric water content in soil and K_a is the soil apparent permittivity given in Eq. 8.

2.2.2 EC estimation from Attenuation

RF techniques measure the signal attenuation $e^{\alpha d}$ through a known distance d to estimate the attenuation coefficient α and then use α to estimate EC. In attenuation-based EC estimation methods, since both the imaginary component of permittivity $\varepsilon_r^{''}$ and electrical conductivity σ contribute to the attenuation, a term apparent conductivity or effective conductivity is used for the EC estimated by such methods, which is given as:

$$\sigma_a = \sigma + 2\pi f \varepsilon_0 \varepsilon_r^{''} \tag{12}$$

which can be calculated from Eq. 3. When $\sigma_a / 2\pi f \varepsilon_0 \varepsilon_r^{'}$ is a small value, the calculation of σ_a can be simplified to

$$\sigma_a = \frac{\alpha \sqrt{\varepsilon_r^{'}}}{60\pi} \tag{13}$$

2.2.3 Limitations of Existing RF Sensing Techniques

Accurate ToF and signal attenuation measurements are the key factors for the accuracy of soil moisture and EC estimation, which imposes a need of special system design to give reliable results. The cost of RF sensing systems is thus usually very high, of the order of several thousand dollars. ToF estimation requires ultra-wide bandwidth to obtain good performance. The bandwidth of systems like GPRs usually spans multiple GHz. Such systems also require specially designed hardware to allow operation on a wide bandwidth. The FCC-imposed power limit for ultra-wideband systems, which is -41.3 dBm/MHz, gives rise to higher power efficiency requirement in designing these systems.

Since EC estimation requires absolute amplitude measurements, it makes the system complex. One needs to know system parameters both during design and in operation. For TDR systems that use transmission line to estimate permittivity and EC, tradeoff exists when choosing probe design parameters for ToF and EC [14]. In antenna-based systems like GPRs, besides the system parameters given in Eq. 5, the whole propagation path from transmitter to receiver, which includes multiple reflections and refractions, also needs to be carefully modeled.

3 SMURF Design

SMURF measures soil moisture and EC only using Wi-Fi signals. A Wi-Fi transmitter, such as a phone or on a tractor, transmits packets which are received by multiple antennas in soil, as shown in Figure 1. All antennas are connected to a single radio. The received signal is used to estimate the permittivity of soil, which is then used to determine the soil moisture and soil EC.

We describe these techniques in detail in the rest of this section.

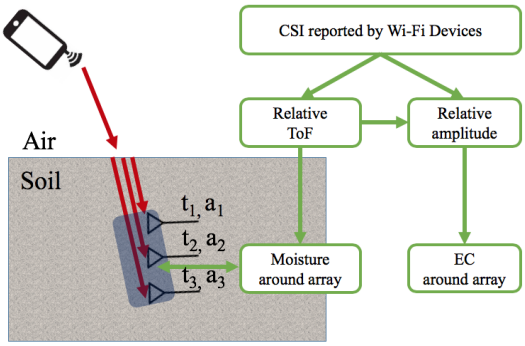

Figure 1: Overview of SMURF

3.1 Estimating Permittivity with Wi-Fi

Overcoming bandwidth limitation using multiple antennas: Antennas and RF chains on a MIMO capable Wi-Fi device are synchronized in time and frequency. Previous work [15, 16, 17] has shown that such antennas can be utilized to estimate angle of arrival (AoA) based on path difference across antennas on an array. In air, this path difference, Δl, corresponds to a delay of $\Delta\tau = \Delta l / c$, where c is the speed of light.

Our insight here is: if the path difference happens in soil, this delay will be longer due to slower wave velocity. Similar to our previous analysis, permittivity can be calculated from Eq. 10. The difference is that the ToF τ in Eq. 10 is no longer the absolute ToF of a signal that travels from the transmit antenna to the receive antenna, but the ToF difference from between multiple receive antennas. In the following discussion, we use the term of relative ToF to refer to the delay caused by the path difference between two adjacent antennas on the array.

Unlike absolute ToF, the accuracy of relative ToF is dominated by the carrier frequency instead of bandwidth. Hence it is possible to get better resolution for relative ToF than absolute ToF.

Mapping relative ToF to soil permittivity: The other key insight in SMURF is that the multiple antennas can be placed to create a path difference in soil, such that the relative ToF maps to permittivity. Typically, we are interested in a scenario where the transmitter is in air and the receiver antenna array is in soil. Since commodity Wi-Fi devices usually have three antennas, we consider using three antennas as the receive array. Next we will show how to estimate permittivity based on relative ToF estimation in this setup.

We use the air-to-soil wave propagation model as shown in Figure 2 to help explain the relationship between relative ToF and path difference in soil. For simplicity, we introduce the concept refractive index n to describe the slow down effect of soil, which relates to the permittivity as follows:

$$n = \sqrt{K_a} \tag{14}$$

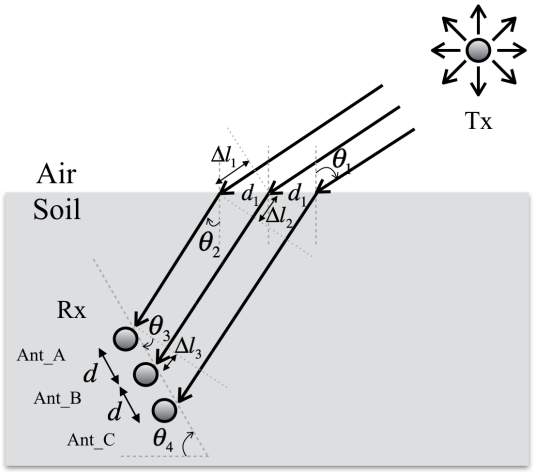

Figure 2: Model of plane wave propagating through air-to-soil surface. Transmit and receive antennas are oriented perpendicular to the plane of the paper. The wave travels to antenna B has a delay of $n\Delta l_2/c + n\Delta l_3/c - \Delta l_1/c$ relative to the wave travels to antenna A.

When signal travels from the transmitter to the receive antennas, the wave is refracted at the air-to-soil surface. Therefore, the path length difference of two adjacent antennas now consists of three parts: $\Delta l_1, \Delta l_2, \Delta l_3$. Δl_1 and Δl_2 are near the surface, while Δl_3 is near the antenna array. Since the speed of wave in soil is c/n, the additional time it takes to travel these path length differences, i.e., relative ToF, is

$$\Delta\tau = \frac{\Delta l_1}{c} - \frac{n\Delta l_2}{c} + \frac{n\Delta l_3}{c} = \frac{\Delta l}{c} \tag{15}$$

where $\Delta l = \Delta l_1 - n\Delta l_2 + n\Delta l_3$ is the equivalent total distance difference. As we can see, Δl contains information of soil refraction index, n. Next, we calculate Δl to find out its relationship with n, and then soil permittivity ε.

$\Delta l_1, \Delta l_2$ and Δl_3 are given as

$$\Delta l_1 = d_1 sin\theta_1, \Delta l_2 = d_1 sin\theta_2, \Delta l_3 = d sin\theta_3 \tag{16}$$

where d is the distance between antennas on the antenna array, d_1 is the distance between waves going to the antenna array at the air-to-soil surface, θ_1 is the angle of incidence, θ_2 is the angle of refraction, θ_3 is the angle of incident wave at the antenna array.

The refraction at air-to-soil surface follows Snell's law, so θ_1 and θ_2 have the following relationship

$$sin\theta_1 = nsin\theta_2 \tag{17}$$

Therefore, we have $\Delta l_1 = n\Delta l_2$ so that $\Delta l = n\Delta l_3 = ndsin\theta_3$. θ_3 is a function of the angle of refraction and the angle of antenna array, θ_4

$$\theta_3 = \theta_4 - \theta_2 \tag{18}$$

We can then rewrite Δl as

$$\Delta l = ndsin(\theta_4 - \theta_2) = ndsin(\theta_4 - arcsin(\frac{sin\theta_1}{n})) \tag{19}$$

In the above equation, d and θ_4 are parameters we can control during the deployment of the antenna array, which are independent of soil moisture. θ_1 depends on the location of transmit antenna and n. Note that in the case of normal incidence, θ_1 is 0 and is independent of n. If we can further know Δl or the corresponding relative ToF $\tau = \Delta l/c$, we can estimate n and K_a.

3.2 Estimating EC from Relative Amplitude

As discussed in Section 2, measuring EC from absolute RF amplitude measurements is prone to errors, and difficult to implement and calibrate. Instead we propose a new technique that uses the ratio of amplitudes across multiple antennas, which we call the relative amplitude, to estimate the EC. This avoids the need to calibrate several other parameters, such as antenna gains, impedance, etc.

Reducing model complexity by exploiting relative amplitude: When wave travels from air into soil, the signal power attenuation is modeled as follows [18]:

$$\frac{P_t}{P_r} = \underbrace{T}_{\text{refraction}} \underbrace{\frac{1}{G_t G_r}}_{\text{antenna gains}} \underbrace{\left(\frac{4\pi(d_s\sqrt{K_a} + d_a)f}{c}\right)^2}_{\text{spreading loss}} \underbrace{e^{2\alpha d_s}}_{\text{transmission loss}} \tag{20}$$

where d_s and d_a are the distances the wave travels in soil and air. T is the transmission coefficient caused by the refraction at air-to-soil interface, which is a function of incident angle and soil permittivity. We notice that for three closely-located and orientation-aligned antennas, their values of T are similar. Furthermore, since soil moisture does not vary much within a small area, the three antennas experience similar impedance change and hence have similar receive gains G_r. G_t is the same for the three antennas since they simultaneously receive the same packet from the same transmitter.

Therefore instead of looking at the absolute amplitude, we propose to use the difference between attenuation of two antennas at different depths, i.e., relative attenuation:

$$\frac{P_r(d_{s_1}, d_{a_1})}{P_r(d_{s_2}, d_{a_2})} = \left(\frac{d_{s_2}\sqrt{K_a} + d_{a_2}}{d_{s_1}\sqrt{K_a} + d_{a_1}}\right)^2 e^{2\alpha(d_{s_2} - d_{s_1})} \tag{21}$$

Comparing the above equation with Eq. 20, the relative amplitude eliminates a lot of system parameters and is less vulnerable to the transmit antenna's location change. In the case of normal incident where $d_{a_1} = d_{a_2}$ and far field, the above equation can be reduced to $P_{rel}(\Delta d) = e^{2\alpha\Delta d}$.

Recall that in Eq. 17, the large values of n in soil limit the angle of refraction to be small. This indicates that d_{s_i} can be approximated to the depth of the ith antenna, which is known

during the deployment of the receive antenna array. Therefore, we can use the relative amplitude or relative power at two antennas at different depths to estimate the attenuation coefficient and then figure out the EC value from Eq. 3 or Eq. 13.

3.3 Soil-Specific Antenna Array Design

To make a good estimation of soil moisture from the relative ToF, we need to carefully choose antenna array parameters that are included in (19). Specifically, these parameters are: (*i*) antenna distance, d, (ii) antenna array rotation θ_4, and (*iii*) angle of incident wave, θ_1. Additionally, we need to choose a proper frequency band as the wave's carrier frequency.

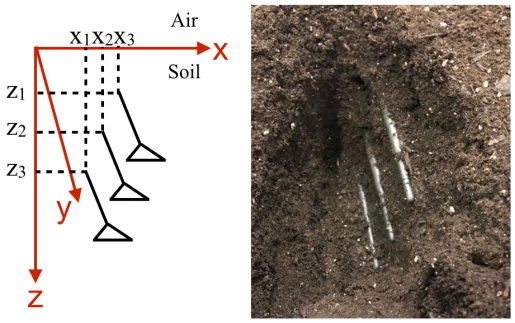

Figure 3: A typical antenna array setup in soil. The three antennas are at put different depths and the distance between two adjacent antennas in the horizontal plane is small.

3.3.1 Array Parameters Selection

In practice, the refractive index of soil, n, is usually a value between 2 and 6, which makes θ_2 a small value (usually below 10 degrees) according to Snell's law. This implies that when the wave is incident on the soil surface, the incident point of the shortest path is usually around the area right above the receiver antennas. Given an antenna distance of d, the distance between the incident points of waves that go to different antennas is around $dcos\theta_4$.

All the equations in Section 3.1 are based on the assumption that soil is a homogeneous medium and the surface is totally flat. However, the real world soil surface is always rough and soil moisture can vary even within a small area. A depth variation of Δd will lead to a ToF variation of $n\Delta d/c$. Consider $\Delta d = 0.01m$ and $n = 3$, the ToF variation is 0.1 ns. If we use a carrier frequency of 2.4 GHz, the phase difference caused by this variation is 0.48π. To reduce the effect of soil non-homogeneity, ideally we want $dcos\theta_4$ to be as small as possible, i.e., either d or $cos\theta_4$ needs to be small. In practice, d needs to be a relatively big value to tolerate variations caused by soil heterogeneity and reduce possible reflections from nearby antennas. Since θ_2 is a small value in soil, setting θ_4 to be 90 degrees is likely to cause blockage of the bottom two antennas' line-of-sight (LoS) paths. Therefore, we choose θ_4 to be a value around 90 degrees that does not cause blockage.

Figure 3 shows a real world example of an antenna setup in soil. Antenna distances in the x-axis are set to be the same so that $\Delta x = x_3 - x_2 = x_2 - x_1$. Additionally, Δx is set to be a small value to reduce the effect of soil non-homogeneity. Antenna distances in the z -axis are also set to be the same so that $\Delta z = z_3 - z_2 = z_2 - z_1$. The depth difference, Δz, is set to be a relative big value to tolerate possible variations in soil structure.

3.3.2 Frequency Band Selection

As we can see from Eq. 20, signal attenuation in soil is frequency-dependent. Higher frequency signals have higher attenuation. Therefore, we should choose a frequency that can at least penetrate to the bottom antenna in our setup.

To understand how Wi-Fi frequency bands perform in soil at different moisture levels, we conducted measurements with a network analyzer in potting soil. Since frequency below 1 GHz is known to have good performance in GPR applications, here our main focus is to look at signal attenuation at Wi-Fi frequency bands, i.e., 2.4 GHz and 5 GHz. Figure 4 plots the signal attenuation in soil for the three receive antennas at depths of 5 cm, 10 cm and 15 cm in soil. With a transmission power of 15 dBm, the channels measured with smaller than -90 dB log magnitude do not contain useful phase information. We can see that the attenuation at 2.4 GHz channels maintain larger than -80 dB log magnitude at all moisture levels while 5 GHz channels do not have good signal strength for the bottom antenna even when soil is very dry. Therefore, although 5 GHz channels have a total bandwidth span of about 665 MHz, the attenuation problem makes most of the data measured at 5 GHz invalid. These results indicate that we should focus on using 2.4 GHz channels, which have about 70 MHz of available bandwidth.

3.4 Dealing with Multipath

The equations derived in Section 3.1 only consider the shortest path from the transmit to the receive antennas. In practice, channels always consist of multiple paths. In our measurement setup, the shortest path is also the strongest path in most cases. Therefore, we use the MUSIC algorithm to accurately recover the shortest path from a multipath channel.

In multipath environment, the CSI of m^{th} antenna and n^{th} frequency can be written as the sum of L paths

$$h_{m,n} = \sum_{l=1}^{L} a_{l,m} e^{-j2\pi(f_0+\Delta f n)\tau_{l,m}} \tag{22}$$

where $a_{l,m}$ is the complex amplitude of l^{th} path, τ_l is the

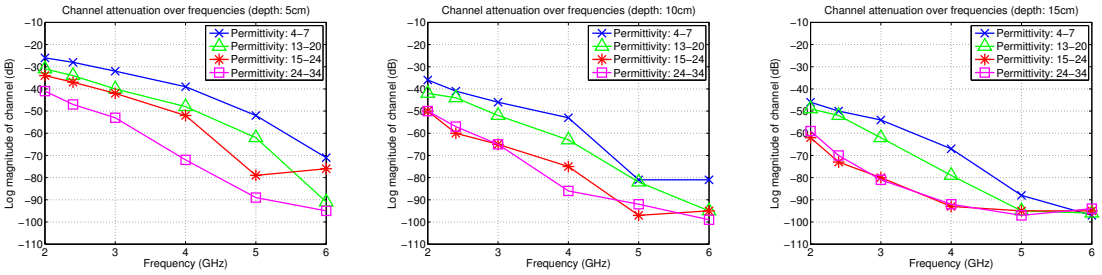

(a) (b) (c)

Figure 4: Channel attenuation in soil at different depths measured by network analyzer. Generally, signal attenuation increases as frequency, depth, or soil moisture increases.

absolute ToF of l^{th} path and Δf is the frequency spacing between two adjacent frequency samples.

If there is no time and frequency synchronization between the transmitter and the receiver, the measured CSI is corrupted with packet detection delay (PDD), sampling frequency offset (SFO), and carrier frequency offset (CFO) introduced by hardware, so the CSI becomes

$$\hat{h}_{m,n} = \sum_{l=1}^{L} a_{l,m} e^{-j\theta_0} e^{-j2\pi(f_0+\Delta f n)(\tau_{l,m}+\tau_0)} \tag{23}$$

where θ_0 is the phase shift caused by CFO and τ_0 is the ToF shift caused by PDD, SFO, and other possible delays in hardware. θ_0 and τ_0 are the same across all the paths, subcarriers in a single channel, and antennas when the samples are measured at the same time.

Note that although we do not know what τ_0 is, we are still able to get the relative ToF between two antennas, $\tau_{l,i} - \tau_{l,j} = (\tau_{l,i} + \tau_0) - (\tau_{l,j} + \tau_0)$. For a uniform linear antenna array, the path difference remains the same for all adjacent antenna pairs under far-field assumption so that the relative ToF also remains the same, i.e., $\Delta\tau_l = \tau_{l,i} - \tau_{l,i+1} = \tau_{l,i+1} - \tau_{l,i+2}$. Therefore, we can use MUSIC to jointly estimate absolute ToF $(\tau_{l,m} - \tau_0)$ and relative ToF $(\tau_{l,i} - \tau_{l,j})$ in a similar way as Spotfi [15] did. Here the absolute ToF refers to the total ToF consisting of PDD, SFO, and delays in hardware. However, Spotfi assumes the phase difference caused by the additional path difference is the the same for all subcarriers, which requires $2\pi B\Delta\tau$ to be a small value, where B is the total bandwidth of N subcarriers. This is not true in our system since we use a larger bandwidth and look at a longer relative ToF. Considering an antenna array with 3 antennas, we construct a modified smoothed CSI matrix without smoothing CSIs of different antennas as follows:

$$\begin{bmatrix} h_{1,1} & h_{1,2} & h_{1,3} & \dots & h_{1,K} \\ \vdots & \vdots & \vdots & \ddots & \vdots \\ h_{1,N-K+1} & h_{1,N-K+2} & h_{1,N-K+3} & \dots & h_{1,N} \\ h_{2,1} & h_{2,2} & h_{2,3} & \dots & h_{2,K} \\ \vdots & \vdots & \vdots & \ddots & \vdots \\ h_{2,N-K+1} & h_{2,N-K+2} & h_{2,N-K+3} & \dots & h_{2,N} \\ h_{3,1} & h_{3,2} & h_{3,3} & \dots & h_{3,K} \\ \vdots & \vdots & \vdots & \ddots & \vdots \\ h_{3,N-K+1} & h_{3,N-K+2} & h_{3,N-K+3} & \dots & h_{3,N} \end{bmatrix} \tag{24}$$

Resolving Ambiguity in Relative ToF: We first explain the reason for the ambiguity issue and then discuss the method to remove it. When wave propagates at a carrier frequency of f, its phase variation is given by

$$\theta = -2\pi f\tau \tag{25}$$

where τ is the ToF. The time it takes the phase to rotate 2π is $\tau_0 = 1/f$. Assuming that the relative ToF of antennas at different depths is Δ, we get the phase of the three receive antennas at three depths as: $\theta_1 = -2\pi f\tau$, $\theta_2 = -2\pi f(\tau + \Delta\tau)$ and $\theta_3 = -2\pi f(\tau + 2\Delta\tau)$. Due to phase ambiguity, we have:

$$\begin{aligned} \theta_1 &= -2\pi f\tau \\ \theta_2 &= -2\pi f(\tau+\Delta\tau) = -2\pi f(\tau+(\Delta\tau+\tau_0)) \\ &= -2\pi f(\tau+(\Delta\tau+2\tau_0)) = \dots \\ \theta_3 &= -2\pi f(\tau+2\Delta\tau) = -2\pi f(\tau+2(\Delta\tau+\tau_0)) \\ &= -2\pi f(\tau+2(\Delta\tau+2\tau_0)) = \dots \end{aligned} \tag{26}$$

From the above equation, we can see that a delay of $\Delta\tau$ is equivalent to $\Delta\tau+\tau_0, \Delta\tau+2\tau_0, \dots$. Thus we will get an infinite number of possible relative ToF values with a separation of τ_0. In 2.4 GHz channels, τ_0 is about 0.4 ns.

Next we show how SMURF leverages the knowledge of soil properties to remove this ambiguity. First, we know that the refraction index in soil is usually between 2 and 6. Therefore, when we set the antenna depth distance at a known value, e.g., 4.5 cm, we know the relative ToF range is 0.3-0.9 ns. In 2.4 GHz, if the relative ToF falls in 0.3-0.5 ns or

0.7-0.9 ns, ambiguity occurs. Now recall that in Figure 4, we have observed a big channel attenuation gap between the two permittivity ranges corresponding to the two ambiguity values. Although multipath and the rotation of transmit antenna may affect the signal strength, we use the signal strength of the three antennas and the data collected at different transmit antenna locations to make a correct choice of antenna pairs to use for relative ToF.

4 Implementation

We implemented SMURF on multiple platforms including USRP, WARP, Intel Wi-Fi Link 5300 NIC, and Atheros AR9590 Wi-Fi NIC to measure soil moisture and EC at 2.4 GHz. USRP allows us to do wideband experiments for ground truthing. The WARP board allows us to replicate CSI measurements similar to Wi-Fi cards, and microbenchmark the performance of SMURF. We validate our results by implementing SMURF on two off-the-shelf Wi-Fi cards.

USRP N200 devices with SBX daughterboards can operate on 400-4400 MHz, however, we observe that the transmission power of the SBX daughterboards drops as frequency increases. Therefore, we only use a bandwidth that spans from 400 MHz to 1400 MHz in our measurements. We use one USRP device as transmitter and the other as receiver. To emulate a MIMO capable receiver equipped with multiple antennas as described in Section 3, we switched antennas during the measurements. For each antenna, the system sweeps through the 400-1400 MHz bandwidth with a step size of 5MHz. To allow such an emulation, PLL offsets, CFO, SFO, and PDD should be consistent for all the receiver antennas. We employ two features on USRP to eliminate PLL offsets, CFO and SFO: (*i*) SBX daughterboards have a PLL phase offset resync feature to synchonize PLL phase offsets on two USRPs after each frequency retune; (*ii*) Two devices can be connected with a MIMO cable to get time and frequency synchronization. To reduce the effect of PDD, we use a narrowband sinusoid to estimate CSI.

WARP boards and the Wi-Fi cards are both MIMO capable and can operate on 2.4 GHz and 5 GHz. With these two types of devices, we consider a more general case that the transmitter and receiver do not share oscillators. How to extract valid CSI information from PLL offsets, CFO, SFO, and PDD corrupted CSI data is the key challenge here. The Intel Wi-Fi cards have a well known issue of random phase jumps at 2.4 GHz [17] while WARP boards and the Atheros cards do not have such an issue. Since WARP has better support for manual configuration, especially gain settings, we evaluated SMURF's performance mainly with WARP. We use a fixed transmit power of 8 dBm in all the experiments, which is much lower than the FCC-imposed power limit for 2.4 GHz channels. To investigate the possibility of using Wi-Fi cards to achieve the same performance as WARP, we set the Wi-Fi cards into monitor mode using the open-source CSI tools[19, 20] on Linux.

We use the entire 70 MHz bandwidth at 2.4 GHz spectrum to cope with potential multipath and amplitude variations that occur due to soil heterogeneity and antenna impedance change. To use the entire bandwidth, we switch across the channels. Therefore, we need to compensate for hardware impairments that lead to inconsist measurements across channels. The calibration on WARP has two procedures. First, we calibrate the PLL phase offsets across channels by leveraging a key observation: although PLL phase offsets are different at different channels, they are constant after a frequency retune. Therefore, the PLL phase offsets at all the channels can be calibrated at the same time and do not need re-calibration unless nodes are reset. Then we adopt the phase sanitization algorithm in SpotFi [15] to equalize the impact of PDD and SFO on channel phase slopes across multiple channel measurements. For Wi-Fi cards, since the RF chains share the same PLL, their random phase behaviour is simpler than WARP, which only has two possible states separated by π.

(a) (b) (c)

Figure 5: Soil measurement setup for multi-antenna system. Antennas are at different depths in soil while there is a rod coming out from soil surface to indicate the location of antenna array in soil. (a) Antennas protected by a waterproof box. (b) Tent with soil boxes. (c) Measurement setup on a farm.

As depicted in Figure 5, we use a waterproof box to protect the connectors of antennas as well as hold antennas at different depths in soil, and there is a rod coming out from soil surface to tell the farmers where the antennas are buried. We setup potting soil boxes in a tent to conduct measurements with controlled salinity and moisture levels, and test real soils in outdoor environments.

5 Performance Evaluation

We first show the accuracy of SMURF in measuring relative ToF, and then evaluate its performance in measuring soil permittivity, EC, and moisture. We use wideband USRP to measure ground truth, and Wi-Fi based measurements on WARP to microbenchmark SMURF. We also present results using Intel and Atheros Wi-Fi cards.

5.1 Relative ToF Estimation Accuracy

SMURF is able to accurately estimate soil moisture and EC with limited bandwidth in 2.4 GHz Wi-Fi. Here we show that

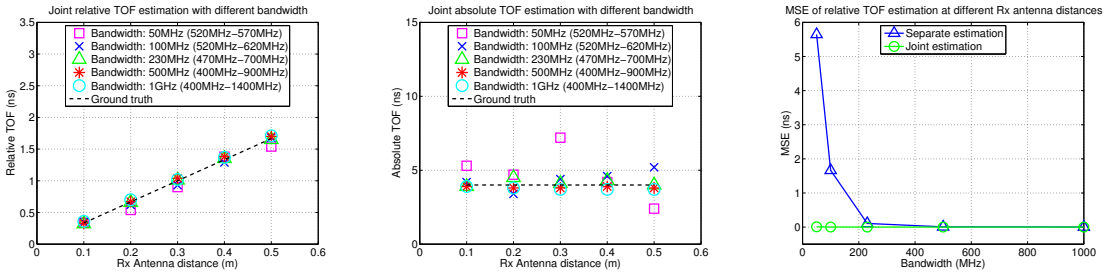

(a) (b) (c)

Figure 6: Performance of the multi-antenna system in estimating relative ToF. (a) Joint relative ToF estimation. Using 3 antennas to jointly estimate relative ToF and absolute ToF give very accurate results even with small bandwidth.(b) Joint absolute ToF estimation for the antenna closest to the transmit antenna. Smaller bandwidth deviates more in estimating absolute ToF. (c) MSE of relative ToF estimation with different bandwidth. The joint estimation method outperforms separate estimation at small bandwidth.

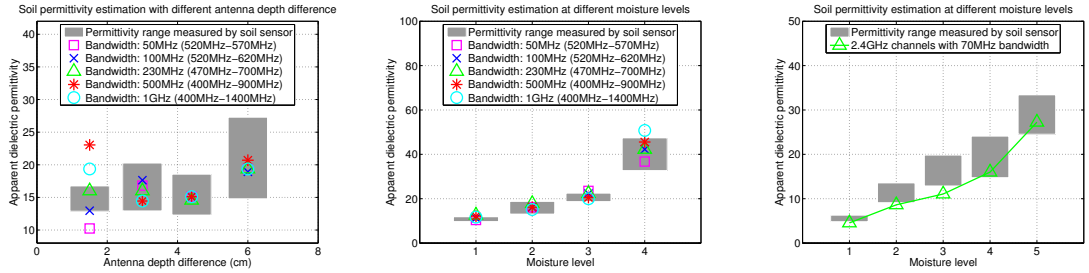

(a) (b) (c)

Figure 7: Soil dielectric permittivity estimation based on relative ToF. (a) Permittivity estimation from USRPs with different antenna depth differences. A small depth difference results in large estimation error. (b) Permittivity estimation with USRPs at different moisture levels. The system can accurately estimate soil moisture value at all soil moisture levels. Even a small bandwidth performs well in distinguishing soil moisture levels. (c) Permittivity estimation with WARPs at different moisture levels. Permittivity estimated from 2.4 GHz channels is generally smaller than the sensor data.

with a few antennas at the receiver, the relative ToF estimation is very accurate even with a very small bandwidth. We first use USRP over a large bandwidth to micro-benchmark, and then use WARP to evaluate the performance at 2.4 GHz channels.

5.1.1 Time-of-Flight Accuracy over the Air

Soil is not a homogeneous medium, and its variations can introduce shifts in estimated ToF. Therefore, we use over-the-air measurements to evaluate the system's performance in estimating absolute ToF. The ground truth ToF is the distance of antennas measured by tape measure and divided by speed of light. We conducted measurements with USRPs by varying the distance between adjacent receive antennas from 0.1 m to 0.5 m. The distance between the transmit antenna and the receive antenna closest to it is 1.2 m and remains the same across all the measurements.

Figure 6 plots the relative ToF and absolute ToF estimation results given by the joint estimation method and the separate estimation method. Relative ToF refers to the ToF difference between two adjacent antennas. The separate estimation method refers to first estimating absolute ToFs at the three antennas separately from the CSI collected by the three receive antennas and then calculating the relative ToF from the average difference of absolute ToFs. The joint estimation method estimates relative ToF and absolute ToF at the same time for the three antennas. Surprisingly, with the joint estimation method, even a bandwidth of 50 MHz gives accurate relative ToF results, although its absolute ToF estimation can deviate more from the ground truth. Furthermore, the joint estimation method has a much smaller MSE of relative ToF and absolute ToF estimation than the separate estimation with small bandwidth.

5.1.2 Relative Time-of-Flight Accuracy in soil

Here we examine the relative ToF estimation performance of the multi-antenna system in soil. We conducted the experiments in potting soil in indoor environment. In the USRP experiments, the transmit antenna is set at a height of 1.08m above soil surface, the receive antennas are put at different depths in soil. In the WARP experiments, the transmit antenna is 0.36m above soil surface. We compare our results with the permittivity measured by a Decagon GS3 soil sensor, which can simultaneous measure permittivity, EC and

temperature. In each experiment, we use the soil sensor to measure moisture at more than 10 locations in the area around the antenna array to account for heterogeneity of soil.

Impact of antenna depth separation: As discussed in 3.3.1, the choice of antenna depth separation is the key factor that affects the relative ToF estimation accuracy in our antenna array design. We conducted experiments with USRPs to examine the impact of depth difference. Figure 7(a) plots the permittivity estimated from relative ToF when antennas have different depth separation. Sensor data shows that soil moisture can vary within a certain range in an area. With a depth separation of 1.5 cm, the estimated permittivity can deviate a lot from sensor data. The reason is the depth separation of 1.5 cm is relatively small compared to possible path length variations that exist in soil due to the heterogeneous nature of soil. With larger antenna depth separation, the permittivity values estimated by different bandwidth are more converged.Based on the results shown in Figure 7(a), we choose an antenna depth separation of 4.5 cm to evaluate the performance of USRP and WARP in the following discussions.

(a) Potting mix (b) Sandy loam (c) Silt loam

Figure 8: Soils used in experiments

Relative ToF at different moisture levels: We vary the soil moisture by adding water, and measure the accuracy of SMURF in determining different soil moisture levels. In each trial, we stir the soil thoroughly to mix water into soil before burying the antenna array. Figure 7(b) shows USRP's performance at different moisture levels and with different bandwidths. The estimated ToF does not deviate too much from sensor data at all moisture levels even with a small bandwidth. We can see the results at the highest moisture level diverge more than the others. This is because larger soil permittivity causes more attenuation of received signal strength, so that the CSIs are less accurate due to low SNRs.

Figure 7(c) shows the estimated permittivity at 2.4 GHz measured by WARP with a bandwidth of 70 MHz. Estimated permittivity increases as moisture level increases. However, the estimated permittivity values are slightly smaller than sensor measurements. This is because of the frequency dependence of soil permittivity. We will discuss this variation later in this section.

5.2 Joint Permittivity and EC Estimation

We now evaluate SMURF's performance in estimating EC. Since SMURF's EC estimation method requires us to first estimate permittivity, here we look at the overall performance including both EC and permittivity. Since controlling EC of soil is non-trivial, we measure the performance of SMURF at different salinity levels of soil, for different soil types. We conduct experiments in potting soil with three different salinity levels and also evaluate SMURF's performance in two types of real soil – sandy loam and silt loam. The sandy loam soil we test is located in a landscaping area near office buildings and the silt load soil is in a real farm. The three types of soils are shown in Figure 8.

We conduct measurements with WARP at 2.4 GHz and the Decagon GS3 soil sensor. For each data point in Figure 9, we average the results of WARP at multiple heights of the transmit antenna from 0.15 m to 0.6 m and the results of the soil sensor at more than 10 locations around the antenna array. Soil moisture, soil solution, and soil type are three major factors that affect EC. We analyze their impacts on EC separately in the following discussion.

EC at different moisture levels: EC has a strong correlation with soil water content. Previous studies [21] have observed a linear relationship between permittivity and EC. Here we examine whether this relationship holds true in our system by varying soil moisture. The tap water we add into soil has a EC value of 0.006 S/m, which is measured by the Decagon GS3 soil sensor. Figure 9(a) plots EC versus permittivity measured by SMURF at 2.4 GHz. EC of all tested soil types tends to increase as permittivity increases. We observed similar trends in permittivity and EC values measured by the soil sensor as shown in Figure 9(b).

In practice, EC readings need to be normalized for different soil moisture values, to make EC maps reliable and repeatable [22]. To enable normalization, the EC-permittivity relationship needs to be a one-to-one function. From this perspective, SMURF outperforms the soil sensor. As shown in 9(b), the curves overlap in the high permittivity region, which means, that the same point in the high permittivity region can map to multiple EC values in the low permittivity region. In contrast, the one-to-one mapping is consistent in SMURF even in the high permittivity region. The poor performance of the soil sensor at high permittivity range is because it is a capacitance sensor and its capacitance measurement is affected by its resistive part while its EC measurement that relies on resistance is accurate. When resistance or EC of soil is high, the sensor will measure a higher capacitance and hence a higher permittivity than the true value.

EC at different salinity levels: EC isolated from moisture variation can be converted to salinity, which has crucial meanings in precision agriculture. Here we evaluate SMURF's capability of detecting different salinity levels of soil. We create three salinity levels by adding different

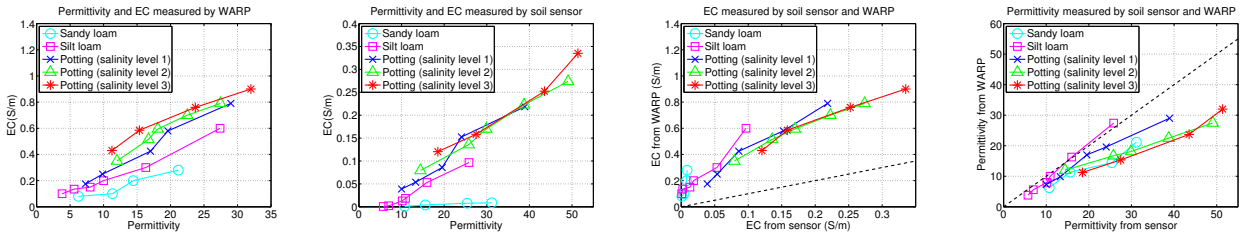

(a) (b) (c) (d)

Figure 9: Soil permittivity and EC estimation for different soil types and salinity levels. (a) Permittivity and EC measured by WARP with 2.4 GHz channels. EC increases as moisture level increases and salinity level increases. (b) Permittivity and EC measured by soil sensor at 70 MHz. EC level affects the soil sensor's permittivity estimation accuracy. (c) Comparison between EC measured by soil sensor and WARP. EC measured at 2.4 GHz is higher than EC measured by soil sensor. (d) Comparison between permittivity measured by soil sensor and WARP. WARP results of different soil types deviate from the soil sensor differently. The deviation is larger at higher salinity levels.

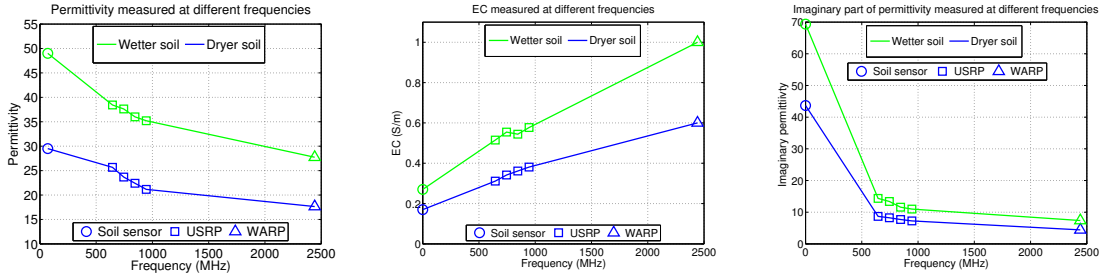

(a) (b) (c)

Figure 10: Permittivity and EC measured by soil sensor, USRP and WARP at different frequencies. (a) Apparent permittivty drops as frequency increases. (b) EC increases as frequency increases. (c) Imaginary effective permittivity converted from EC.

amount of salt into three boxes with the same type of potting soil. By looking at EC values vertically with the same permittivity in Figure 9(a) and Figure 9(b), we observe that SMURF can successfully detect the increase of salinity levels from EC readings at all permittivity regions while the soil sensor can only tell the difference of salinity levels when permittivity is smaller than 20.

EC in different soils: Different soil types may have different EC-permittivity and EC-salinity relationships due to dielectric property change [23]. Previously, we conducted most of our experiments with potting soil since it is more accessible and hence easier to set up controlled experiments. Here we test two typical types of real soils to show the accuracy of SMURF in detecting permittivity and EC of real world soils. As shown in Figure 9(a) and Figure 9(b), the three types of soils have quite different salinity levels. Generally, SMURF can detect the permittivity increase as water content increases and EC increase as salinity level increases in different types of soils. The rate of increase in EC over permittivity is different for different soil types and even for the same soil type with different salinity levels. In practice, SMURF will need to be calibrated for different soil types, just as the existing soil sensors have to be calibrated before use.

Comparing SMURF with soil sensor: We plot EC measured by SMURF and the soil sensor in Figure 9(c), and permittivity measured by SMURF and the soil sensor in Figure 9(d). Overall, SMURF measures a larger EC value and a smaller permittivity value than the soil sensor. The EC-EC slopes decrease as salinity level increases while the permittivity-permittivity slopes do not have a clear trend. The permittivity deviation is larger at larger moisture levels.

Comparing WARP with Atheros Wi-Fi card: To compare the performance of WARP and Atheros Wi-Fi card, we conduct experiments with the same transmit and receive antenna locations for same soil. Basically, we just change the data transmit and record devices from WARPs to Atheros WiFi cards. We see very similar CSI phase results measured by WARP and Wi-Fi cards. While the Atheros Wi-Fi cards do not give reliable amplitude measurements, we can use its RSSI reported for each channel for EC estimation. We observe that the EC measured by Wi-Fi cards using RSSIs are similar to the EC measured by WARP. One example set of results is: permittivity and EC measured by WARP is 8.8 and 0.24 S/m, while permittivity and EC measured by Wi-Fi is 9.2 and 0.21 S/m.

5.2.1 Understanding Permittivity and EC Deviations between SMURF and Soil Sensor

Previous studies [8, 23, 24, 25] show that both the real and imaginary parts of permittivity of soil are frequency depen-

dent and affected by salinity, where the imaginary permittivity refers to the effective imaginary permittivity given as $\varepsilon_{re}^{''} = \varepsilon_{r}^{''} + \sigma/2\pi f\varepsilon_0$. In the frequency range from a few MHz to Wi-Fi frequency bands at 2.4 GHz, the real and imaginary parts of permittivity both drop over frequency while the imaginary drops more significantly at lower frequencies. As salinity increases, the real permittivity slightly drops while the imaginary permittivity increases and the increase is significant at lower frequencies. The difference of imaginary permittivity at lower frequencies and higher frequencies is due to the EC component $\sigma/2\pi f\varepsilon_0$. To evaluate how SMURF's relative ToF and relative amplitude based permittivity and EC estimation match with existing studies, we conduct experiments with the soil sensor operating at 70 MHz, USRP operating at 400-1400 MHz, and WARP operating at 2.402-2.472 GHz. Both USRP and WARP use the multi-antenna system to measure relative ToF and amplitude. Since USRP measures a wide bandwidth, we are able to get multiple data points by selecting subsets of frequency ranges within 400-1400 MHz.

Figure 10 shows the results of potting soil at two different moisture levels. As frequency increases, the estimated permittivity decreases and EC increases, which agree with the deviations we observe earlier. Note that effective imaginary and effective EC, which is the EC value we measure, are two interchangeable concepts and has a relationship of $\varepsilon_{re}^{''} = \sigma_a/2\pi f\varepsilon_0$. We convert our EC results to imaginary permittivity in Figure 10(c) for a more intuitive comparison with exiting studies. The trends and scale of values of our estimated real and imaginary permittivity match with results reported in [25].

Implications for calibration requirements: The above analysis provides implications about how we should calibrate our system. (i) Getting real part of permittivity from apparent permittivity measurement: as we can see from Figure 10(c), the imaginary permittivity at 2.4 GHz is a small value compared with the real part of permittivity so the measured apparent permittivity is equal to the real part of permittivity and there is no need for calibration. (ii) Estimating soil water content from permittivity: the drop of real permittivity over frequency needs to be calibrated to use the existing water content-permittivity models which are mainly developed for lower frequencies. Fortunately, the dependence of real and imaginary permittivity on frequency has been modeled for different soil types, although measurements are still required to validate those models. (iii) Estimating salinity from measured EC: to get the true EC component, the imaginary permittivity component needs to be removed from the measured apparent EC. On the one hand, we can refer to existing studies of soil dielectric properties to get the imaginary permittivity values for different soil types; on the other hand, our results in Figure 9(a) and 9(c) indicate that it is possible to directly convert our measured EC to salinity.

6 Related Work

While soil sensing using RF has been well studied, our work is the first that makes it possible to use off-the-shelf low-cost Wi-Fi devices for detecting soil properties. We discuss related work in three main categories:

Soil moisture sensing using RF: The well-established RF sensing techniques can be classified into three types. (*i*) Remote sensing techniques[26, 27, 28] use the dependence of soil reflectivity on soil moisture to sense soil moisture. These approaches have low spatial resolution from 1 m to 10s of km and can only detect soil moisture on shallow soil surface with a depth of a few centimeters. (*ii*) ToF-based techniques such as GPR [29] and time domain reflectometry (TDR) [30] provides good spatial resolution. However, these approaches rely on specialized ultra-wideband systems to get accurate ToF estimation, thus are very expensive. (*iii*) A few studies [31, 32, 33, 34] have proposed to use a moisture or EC sensitive sensing element together with a low-cost communication node, e.g., RFID or backscatter, to sense soil. However, low-cost sensing elements like a capacitive sensor can only sensor moisture, not EC, and its accuracy will not be comparable to the more reliable but higher-cost commodity sensors. A specialized probe that is sensitive to moisture and salinity change is used in [32] to detect moisture and salinity, which could potentially increase cost.

AoA and ToF estimation on Wi-Fi devices: We build SMURF on existing AoA and ToF estimation technologies developed for commodity Wi-Fi devices [15, 35, 36, 20, 16, 37]. However, these technologies do not work for wave propagation in soil due to different reasons. The sub-nanosecond accuracy achieved in Chronos [35] is unlikely in soil due to the high attenuation of 5 GHz signals. SpotFi's [35] accuracy benefits from 40 MHz bandwidth and the carrier frequency of 5 GHz. To combat signal attenuation in soil, we instead use 20 MHz channels at 2.4GHz. To deal with multipath in soil and amplitude variations due to impedance change or soil heterogeneity, we spliced all 2.4 GHz channels. However, existing work on channel splicing only works for a single antenna [20, 37]. We utilize our observations about hardware to eliminate exhaustive search for both PLL phase offset calibration [17] and channel splicing [20, 37]

Other low-cost techniques: Other than ultra-wideband systems and Wi-Fi devices, there are some other commercially available RF devices that can provide ToF estimation, such as global positioning system (GPS) receivers [38]. GPS relies on ToF between satellites and the receiver for localization. However, its ToF resolution and penetration depth limit its usage in ToF-based soil moisture sensing. Ranging techniques using ultrasound [39, 40] have been well studied for over the air wave propagation. However, ultrasound is not appropriate for ToF-based soil moisture estimation since it does not correlate very with moisture, which limits its applications of soil sensing to rely on reflectivity[41, 42].

Although there exist hobbyist soil sensors that cost lower than 30 dollars, they are not recommended by agriculture experts for irrigation management on farms [2]. The cheapest suggested soil moisture sensors still cost over 50 dollars. Actually, the higher accuracy of expensive sensors can potentially help to save more water resources in the long term. We note that we are not aware of any commercially available EC sensor below 100 dollars.

7 Discussion & Future Work

SMURF takes the first step in leveraging Wi-Fi communication for estimating soil properties. However, for it to achieve its true potential, where a farmer with any Wi-Fi enabled device can infer soil properties, we plan to take SMURF in the following directions.

Integration with commercial Wi-Fi devices: The Wi-Fi chip vendors in off-the-shelf phones have started to expose CSI information. The Intel and Atheros 11n chipsets have shown the feasibility of providing this information to the user level, and we will work with other chip vendors to expose these values. We note that SMURF only requires a single antenna at the smartphone. Furthermore, since 2.4 GHz of the spectrum is available in nearly all countries, we expect SMURF to be universally usable.

Profiling overhead: In its current implementation SMURF relies on an offline profiling of the ToF and relative ToF values for different soil types. This is similar to how surrogate soil sensing methods are currently used. We however realize that this is an overhead when using these sensors, and could potentially be a source of inaccuracy in unknown soil conditions. We are investigating ways in which the multiple antennas in soil can be used to self calibrate, especially since each pair of antennas can be used as a different measurement to estimate the corresponding soil type.

Sensing deeper in soil: The technique might not work over 2.4 GHz of spectrum for fruit orchards, where the roots might be up to 1 meter deep, and the Wi-Fi signals might not have good SNR at those depths. TV white space spectrum can be used to sense soil at depths deeper than 1 m, which is sufficient for most broadacre crops and for horticulture. While one could still use SMURF over the TV White Space spectrum, we are investigating ways in which Wi-Fi over the 2.4 GHz spectrum could be used as well. Our key insight is to use beamforming to increase the SNR in the direction of the antennas in soil. The challenge of course is that the direction of the beamformed signal will have to change based on the moisture level of soil. We are actively investigating solutions to this problem.

Price: We note that SMURF does not require a specialized reader. Only a Wi-Fi device is needed to communicate with the device embedded in soil. For the device in soil, it is recommended to use a chipset with 3 antennas, although a 2-antenna radio can work as well. The price of a typical IoT board with a Wi-Fi chipset with an onboard ARM processor and batteries is similar to a Vocore2, or C.H.I.P., both of which cost less than 10 dollars.

Battery Life: The device in soil only needs to wake up when the surveying device is closeby. Else, it should operate in deep sleep mode. One way to accomplish this is using the Network List Offload (NLO) feature of Wi-Fi that turns the radio into very low power mode until it hears a beacon with the expected BSSID. In this case, the surveyor can be programmed to pretend like a Wi-Fi Access Point and emit a beacon with a SMURF BSSID.

8 Summary

In this paper we present a new technique, called SMURF, for estimating soil moisture and EC using Wi-Fi signals. The system estimates soil moisture by measuring the relative time of flight of Wi-Fi between multiple antennas, and the soil EC by measuring the ratios of the amplitudes of the signals across different antennas. We have implemented SMURF on two different SDR platforms, and on two Wi-Fi cards. Our results show that SMURF can accurately estimate soil moisture and EC at various depths.

Our vision is to enable a future in which a farmer can take her smartphone, which has a Wi-Fi radio, close to soil and learns about the soil conditions, such as soil moisture and soil EC. By avoiding use of sensors that cost more than 100s of dollars each, SMURF reduces the price for sensing these parameters, thereby taking a big step in enabling the adoption of data-driven agriculture techniques by small holder farmers.

References

[1] Soil electrical conductivity, soil quality kit – guide for educators, usda nrcs.

[2] Soil moisture monitoring: a selection guide, department of primary industries and regional development, government of australia, 5th sep, 2018.

[3] Deepak Vasisht, Zerina Kapetanovic, Jongho Won, Xinxin Jin, Ranveer Chandra, Sudipta N. Sinha, Ashish Kapoor, Madhusudhan Sudarshan, and Sean Stratman. Farmbeats: An iot platform for data-driven agriculture. In *14th USENIX Symposium on Networked Systems Design and Implementation, NSDI 2017, Boston, MA, USA, March 27-29, 2017*, pages 515–529, 2017.

[4] Milton Whitney et al. Instructions for taking samples of soil for moisture determinations. 1894.

[5] EA Colman. The place of electrical soil-moisture meters in hydrologic research. *Eos, Transactions American Geophysical Union*, 27(6):847–853, 1946.

[6] Harrison E Patten. Heat transference in soils. 1909.

[7] LA Richards. Soil moisture tensiometer materials and construction. *Soil Sci*, 53(4):241–248, 1942.

[8] Wilford Gardner and Don Kirkham. Determination of soil moisture by neutron scattering. *Soil Science*, 73(5):391–402, 1952.

[9] Harald T Friis. A note on a simple transmission formula. *Proceedings of the IRE*, 34(5):254–256, 1946.

[10] Harry M Jol. *Ground penetrating radar theory and applications*. elsevier, 2008.

[11] G Clarke Topp, JL Davis, and Aa P Annan. Electromagnetic determination of soil water content: Measurements in coaxial transmission lines. *Water resources research*, 16(3):574–582, 1980.

[12] Kurt Roth, Rainer Schulin, Hannes Flühler, and Werner Attinger. Calibration of time domain reflectometry for water content measurement using a composite dielectric approach. *Water Resources Research*, 26(10):2267–2273, 1990.

[13] John O Curtis. Moisture effects on the dielectric properties of soils. *IEEE transactions on geoscience and remote sensing*, 39(1):125–128, 2001.

[14] DA Robinson, Scott B Jones, JM Wraith, Daniel Or, and SP Friedman. A review of advances in dielectric and electrical conductivity measurement in soils using time domain reflectometry. *Vadose Zone Journal*, 2(4):444–475, 2003.

[15] Manikanta Kotaru, Kiran Joshi, Dinesh Bharadia, and Sachin Katti. Spotfi: Decimeter level localization using wifi. In *ACM SIGCOMM Computer Communication Review*, volume 45, pages 269–282. ACM, 2015.

[16] Jie Xiong and Kyle Jamieson. Arraytrack: a fine-grained indoor location system. Usenix, 2013.

[17] Jon Gjengset, Jie Xiong, Graeme McPhillips, and Kyle Jamieson. Phaser: Enabling phased array signal processing on commodity wifi access points. In *Proceedings of the 20th annual international conference on Mobile computing and networking*, pages 153–164. ACM, 2014.

[18] ZHI Sun, Ian F Akyildiz, and Gerhard P Hancke. Dynamic connectivity in wireless underground sensor networks. *IEEE Transactions on Wireless Communications*, 10(12):4334–4344, 2011.

[19] Daniel Halperin, Wenjun Hu, Anmol Sheth, and David Wetherall. Tool release: Gathering 802.11 n traces with channel state information. *ACM SIGCOMM Computer Communication Review*, 41(1):53–53, 2011.

[20] Yaxiong Xie, Zhenjiang Li, and Mo Li. Precise power delay profiling with commodity wifi. In *Proceedings of the 21st Annual International Conference on Mobile Computing and Networking*, pages 53–64. ACM, 2015.

[21] MA Hilhorst. A pore water conductivity sensor. *Soil Science Society of America Journal*, 64(6):1922–1925, 2000.

[22] Robert Dwight Grisso, Marcus M Alley, David Lee Holshouser, and Wade Everett Thomason. Precision farming tools. soil electrical conductivity. 2005.

[23] Myron C Dobson, Fawwaz T Ulaby, Martti T Hallikainen, and Mohamed A El-Rayes. Microwave dielectric behavior of wet soil-part ii: Dielectric mixing models. *IEEE Transactions on Geoscience and Remote Sensing*, (1):35–46, 1985.

[24] M Craig Dobson and Fawwaz T Ulaby. Active microwave soil moisture research. *IEEE Transactions on Geoscience and Remote Sensing*, (1):23–36, 1986.

[25] Timo Saarenketo. Electrical properties of water in clay and silty soils. *Journal of Applied Geophysics*, 40(1-3):73–88, 1998.

[26] JR Wang and BJ Choudhury. Remote sensing of soil moisture content, over bare field at 1.4 ghz frequency. *Journal of Geophysical Research: Oceans*, 86(C6):5277–5282, 1981.

[27] Thomas J Jackson. Iii. measuring surface soil moisture using passive microwave remote sensing. *Hydrological processes*, 7(2):139–152, 1993.

[28] Binayak P Mohanty, Michael H Cosh, Venkat Lakshmi, and Carsten Montzka. Soil moisture remote sensing: State-of-the-science. *Vadose Zone Journal*, 16(1), 2017.

[29] JA Huisman, SS Hubbard, JD Redman, and AP Annan. Measuring soil water content with ground penetrating radar. *Vadose zone journal*, 2(4):476–491, 2003.

[30] K Noborio. Measurement of soil water content and electrical conductivity by time domain reflectometry: a review. *Computers and electronics in agriculture*, 31(3):213–237, 2001.

[31] Azhar Hasan, Rahul Bhattacharyya, and Sanjay Sarma. A monopole-coupled rfid sensor for pervasive soil moisture monitoring. In *Antennas and Propagation Society International Symposium (APSURSI), 2013 IEEE*, pages 2309–2310. IEEE, 2013.

[32] Shuvashis Dey, Nemai Karmakar, Rahul Bhattacharyya, and Sanjay Sarma. Electromagnetic characterization of soil moisture and salinity for uhf rfid applications in precision agriculture. In *Microwave Conference (EuMC), 2016 46th European*, pages 616–619. IEEE, 2016.

[33] Spyridon-Nektarios Daskalakis, Stylianos D Assimonis, Eleftherios Kampianakis, and Aggelos Bletsas. Soil moisture scatter radio networking with low power. *IEEE Transactions on Microwave Theory and Techniques*, 64(7):2338–2346, 2016.

[34] Md Mazidul Islam, Kimmo Rasilainen, and Ville Viikari. Implementation of sensor rfid: Carrying sensor information in the modulation frequency. *IEEE Transactions on Microwave Theory and Techniques*, 63(8):2672–2681, 2015.

[35] Deepak Vasisht, Swarun Kumar, and Dina Katabi. Decimeter-level localization with a single wifi access point. In *NSDI*, pages 165–178, 2016.

[36] Swarun Kumar, Stephanie Gil, Dina Katabi, and Daniela Rus. Accurate indoor localization with zero start-up cost. In *Proceedings of the 20th annual international conference on Mobile computing and networking*, pages 483–494. ACM, 2014.

[37] Jie Xiong, Karthikeyan Sundaresan, and Kyle Jamieson. Tonetrack: Leveraging frequency-agile radios for time-based indoor wireless localization. In *Proceedings of the 21st Annual International Conference on Mobile Computing and Networking*, pages 537–549. ACM, 2015.

[38] Elliott Kaplan and Christopher Hegarty. *Understanding GPS: principles and applications*. Artech house, 2005.

[39] Andy Ward, Alan Jones, and Andy Hopper. A new location technique for the active office. *IEEE Personal communications*, 4(5):42–47, 1997.

[40] Nissanka B Priyantha, Anit Chakraborty, and Hari Balakrishnan. The cricket location-support system. In *Proceedings of the 6th annual international conference on Mobile computing and networking*, pages 32–43. ACM, 2000.

[41] DA Robinson, CS Campbell, JW Hopmans, Brian K Hornbuckle, Scott B Jones, R Knight, F Ogden, J Selker, and O Wendroth. Soil moisture measurement for ecological and hydrological watershed-scale observatories: A review. *Vadose Zone Journal*, 7(1):358–389, 2008.

[42] Nobutaka Hiraoka, Takefumi Suda, Kazuhiro Hirai, Katsuhiko Tanaka, Kazunari Sako, Ryoichi Fukagawa, Makoto Shimamura, and Asako Togari. Improved measurement of soil moisture and groundwater level using ultrasonic waves. *Japanese Journal of Applied Physics*, 50(7S):07HC19, 2011.